RSC Advances

PAPER

View Article Online
View Journal | View Issue

Cite this: *RSC Adv.*, 2020, **10**, 28950

Catalytically active coordination polymer with a tiny Zn_2Se_2 ring bridged by bis-selone†

Mannarsamy Maruthupandi and Ganesan Prabusankar *

Received 23rd May 2020
Accepted 23rd July 2020

DOI: 10.1039/d0ra04577b

rsc.li/rsc-advances

The unprecedented architecture of a one-dimensional coordination polymer with a tiny Zn_2Se_2 ring system incorporated in the hydrogen-bonded array has been prepared, where the di-selone ligand functions as a unique neutral bridging ligand. The coordination polymer shows excellent catalytic activity in substituted 8-hydroxy-2-quinolinyl synthesis through Knoevenagel condensation reaction.

Introduction

Imidazoline selones have been considered as a neutral σ donor ligand that can be an ideal choice to replace the N-heterocyclic carbene (NHC) type ligands in catalysis.[1–4,5a] To date, many metal complexes bearing imidazole selone ligands have been prepared to understand the potential role in catalysis. Since imidazole-2-selones can donate up to six electrons with multiple coordination modes, various coordination patterns have been observed.[5b,5e] Similar such new coordination modes of a multidentate ligand can bring a new strategy to construct novel coordination polymers. Like NHC, imidazole selone ligated metal clusters or polynuclear assemblies are rare due to the steric influence of a N-substituent at imidazole-2-selone.[3] Among transition metal derivatives of imidazole-2-selone, the catalytic application of Zn(II)-imidazole selone is lest studied due to the formation of insoluble ill-defined material.[4–6] The isolation of structurally characterized coordination polymers of Zn(II)-imidazole selone is the most challenging task.[7]

In general, the zinc(II) coordination polymers have demonstrated to their potential applications in catalysis, electrochemistry as conducting materials and optoelectronics.[8] However, only one structural investigation on bis-azole thione bridged zinc(II) coordination polymer has been reported.[4–7] The similar class of zinc selones and their catalytic applications are still in the embryonic stage, and their coordination polymers are particularly rare (Scheme 1). We have reported the first zinc(II) selone, $[\{(\mathbf{L^I})_2Zn\}\{ClO_4\}_2\cdot 2H_2O]$ ($\mathbf{L^I}$ = 3-(2-methoxy-2-oxoethyl)-1-mesityl-imidazoline selone) and $[\{(\mathbf{L^{II}})_4Zn\}^{2+}\{ClO_4\}_2^{2-}]$ ($\mathbf{L^{II}}$ = 1-(2,6-diisopropylphenyl)-3-(2-methoxy-2-oxoethyl)-imidazoline selone) mediated Barbier coupling reactions in aqueous alcohol media.[4] Later we developed the homoleptic and heteroleptic zinc(II) selones, $[Zn(\mathbf{L^{III}})_2X_2]$ ($\mathbf{L^{III}}$ = 1-methyl 3-naphthyl-methyl imidazoline-2-selone), (X = Cl or Br), $[\{Zn(\mathbf{L^{IV}})_4\}\{X'\}_2]$ (X′ = BF_4 or ClO_4), and $[Zn(\mathbf{L^{IV}})_2Br_2]$ ($\mathbf{L^{IV}}$ = 1-isopropyl 3-methylimidazoline-2-selone) catalysed thioetherification of aryl halides.[5] Recently we developed the mesoionic chalcogenone zinc(II) complexes $[(\mathbf{L^V})Zn(Cl)_2(HOMe)]$, $[(\mathbf{L^V})Zn(Br)(\mu^2\text{-}Br)]_2$, $[(\mathbf{L^{VI}})Zn(X)_2(HOMe)]$ (X = Cl or Br), $[(\mathbf{L^{VII}})Zn(Br)(\mu^2\text{-}Br)]_2$ and ($\mathbf{L^V}$ = 1-(2-mesitylene)-3-methyl-4-phenyltriazolin-5-selone; $\mathbf{L^{VI}}$ = 1-(2-mesitylene)-3-methyl-4-phenyl triazolin-5-thione; $\mathbf{L^{VII}}$ = 1-(benzyl)-2-3(methyl)-4-phenyltriazolin-5-selone), for thioetherification reactions.[6] These catalysts were highly active towards the cross-coupling reaction between aryl halides and thiophenols without scrubbing oxygen. However, the

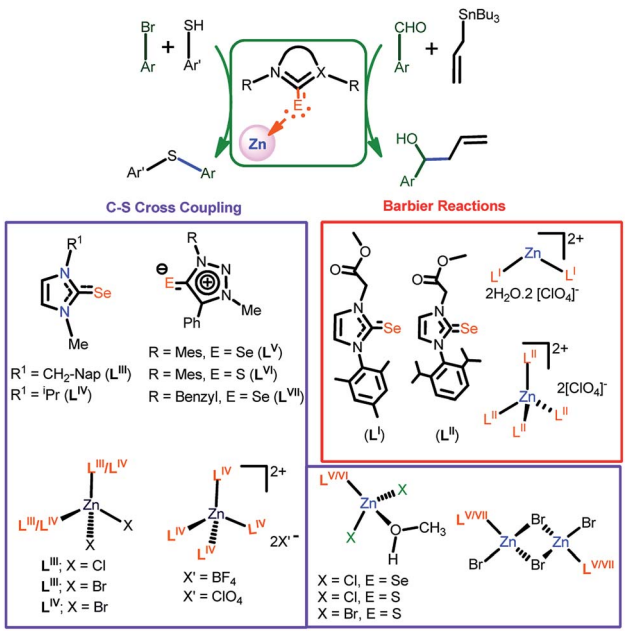

Scheme 1 Known zinc(II) imidazoline chalcogenone mediated catalytic reactions.

Department of Chemistry, Indian Institute of Technology Hyderabad, 502 285, India. E-mail: prabu@iith.ac.in

† Electronic supplementary information (ESI) available: FT-IR, ^{1}H NMR, and ^{13}C NMR spectra along with solid-state packing and sample under UV-vis light of reported molecules. CCDC 2005360 ($\mathbf{L}\cdot H_2O$) and 2005361 (**1**). For ESI and crystallographic data in CIF or other electronic format see DOI: 10.1039/d0ra04577b

application of structurally characterized zinc(II) complexes based on bridging azo-selone ligands are scarce.

Our interest is in the synthesis of new zinc coordination polymers containing bis-selone ligand. To enhance the structural multifariousness, the incorporation of flexible ethyl spacer containing bis-selone into the zinc selone structure is highly desired. This investigation has been based on the notion that modification of the zinc coordination environment may disrupt the overall structure of the zinc coordination polymer, thus altering and/or favoring their catalytic activities. Based on this approach, we reported the largest copper(I) cubanes with pyridine bridged bis imidazole-2-selone.[3] This result shows that the ligand demonstrates a peculiar ability to formulate the cubanes, and the results also indicated that the flexible alkane spacer plays a significant role in directing the cluster structures and topologies. To further investigate the influence of the neutral ligands and alkane spacer on the formation of supramolecular architectures, we focus on synthesizing a new bis-benzimidazole selone ligand, and we report the reaction between $ZnBr_2$ and [(3,3′-ethane)bis(1-isopropyl-benzimidazole-2-selenone)] (**L**), which give rise to a catalytically active 1D coordination polymer $[(\mathbf{L})\{ZnBr_2\}_2]_\alpha$ (**1**). The coordination polymer **1** depicts a new architecture generated by an unusual Zn_2Se_2 ring bridged through the bis benzimidazole selone ligand.

Results and discussion

Synthesis and characterization of $\mathbf{L}\cdot H_2O$ and 1

The selone ligand $\mathbf{L}\cdot H_2O$ was isolated with excellent yield from the reaction between 1,1′-(ethane)bis(3-isopropyl-benzimidazolium) bromide salt with selenium powder in the presence of K_2CO_3 (Scheme 2). $\mathbf{L}\cdot H_2O$ is entirely soluble in MeOH, DCM, $CHCl_3$, and DMSO, while partially soluble in ethyl acetate and insoluble in hexane. The FT-IR spectrum of $\mathbf{L}\cdot H_2O$ exhibits an intense C=Se stretching frequency at 1164 cm^{-1}. In ^{13}C NMR, the carbon attached with selenium (C=Se) appears at 165 ppm. The solid-state structure of $\mathbf{L}\cdot H_2O$ was further confirmed by single-crystal X-ray diffraction technique. The crystallographic data are provided in Table 1. The chalcogenone ligands $\mathbf{L}\cdot H_2O$ crystallized in monoclinic, space group $P2_1/c$. The selected bond lengths and bond angles are listed in Fig. 1. The C=Se bond lengths of $\mathbf{L}\cdot H_2O$ is 1.820(74) Å. The observed C=Se bond length is slightly shorter than that of $\mathbf{L^I}$ (1.835(3) Å), and $\mathbf{L^{II}}$ (1.834(3) Å).[4] The N–C–N bond angle of $\mathbf{L}\cdot H_2O$ indicates the existence of sp^2 hybridization.

The new coordination polymer **1** was synthesized with excellent yield from the reaction between zinc bromide, and $\mathbf{L}\cdot H_2O$. **1** is partially soluble in MeOH, EtOH, and DMSO. The formation of **1** was confirmed by FT-IR, NMR (^1H and ^{13}C), UV-visible, and TGA techniques. **1** crystallized in the monoclinic space group, I_2/a. The crystallographic data for **1** are listed in Table 1. The selected bond lengths and bond angles are assembled in Fig. 2. The solid-state structure of **1** reveals a novel 1D coordination polymer based on the assembling of the Zn_2Se_2 ring.

The obtained coordination polymer consists of a 1 : 1 ratio of Zn(II) ion and selone. The selenium center in **1** is heavily disordered (*vide infra*). The coordination mode of the bis-selenium ligand in **1** is quite rare for zinc(II)-selones. The zinc centers and selenium atoms of the bridging organo selenium ligand are located in the same plane (Φ of Zn1–Se1–Zn1#–Se1#=0°). That is, Zn_2Se_2 shows a synperiplanar conformation. Two selenium atoms of the benzimidazole groups from **L** bridges between zinc(II) center to form a tiny Zn_2Se_2 ring. Owing to the strained chelation of the selone, an extraordinarily small bond angle of 67.42(9)° is observed at Se1–Zn1–Se1, which is not comparable with $[Zn(\mathbf{L^{III}})_2Br_2]$ (102.99(5)°) and $[Zn(\mathbf{L^{IV}})_2Br_2]$ (105.58(11)°).[5a]

Since the ethyl bridge of benzimidazole-2-selone can rotate, **L** acts as a pliable connector between the zinc centers of Zn_2Se_2 rings. Each ligand connects two zinc(II) centers to yield a one-dimensional structure with a small ring cavity (about 4.9 Å) in the *ab* plane (Fig. 3). Interestingly, the zinc center of **1** features a highly distorted tetrahedral structure with the selenium bridging atom in the basal position, and the apical plane positions are occupied by two bromine ligands. The Zn1–Se1 bond lengths (2.494(4) Å) is comparable to the known complex of a similar type, $[Zn_2(\mathbf{L^{III}})_2Br_4]$ (2.476(3) Å and 2.491(3) Å).[5a] The C=Se bond distance in **1** is 1.866(3) Å, which is about 0.046 Å longer than that of **L** due to the good σ donor property of the ligand. The Se(1)=C(1) bond lengths in **1** considerably elongated compared to the corresponding ligand **L**. These one-dimensional coordination polymers interdigitated each other to afford a layered structure through hydrogen bonds between bromine and CH moieties at diselone ligand. **1** shows both intra- and intermolecular Br···H–C hydrogen bonding interactions. These hydrogen bonding interactions connect the 1D coordination polymer to the self-assembled 2D stacking array of a layered structure.

The thermal stability of coordination polymer **1** was investigated using thermogravimetric analysis under a nitrogen atmosphere with a heating rate of 10 °C min^{-1} (Fig. 4). The 1D coordination polymer shows two-step weight loss with very high

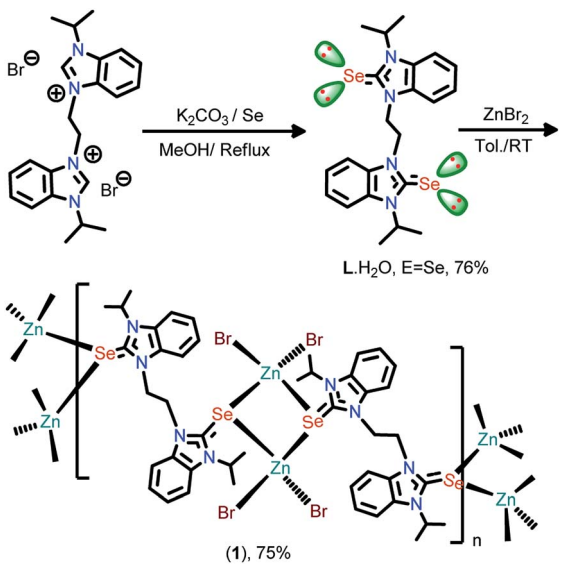

Scheme 2 Synthesis of $\mathbf{L}\cdot H_2O$ and **1**

Table 1 Crystal data and structure refinement parameters for $L \cdot H_2O$ and **1**

	$L \cdot H_2O$	**1**
Empirical formula	$C_{22}H_{26}N_4OSe_2$	$C_{22}H_{26}Br_2N_4Se_{1.69}ZnO_{0.31}$
Formula weight	522.41	710.06
T (K)	293	120.01(10)
Crystal system	Monoclinic	Monoclinic
Space group	$P2_1/c$	$I1_2/a_1$
a (Å)	12.244(5)	17.2917(5)
b (Å)	15.559(5)	9.4210(4)
c (Å)	13.831(5)	16.2331(5)
α (°)	90	90
β (°)	113.152(5)	93.499(3)
γ (°)	90	90
Volume (Å^3)	2422.7(15)	2639.53(16)
Z	4	4
Density (calculated), mg m^{-3}	1.432	1.846
Absorption coefficient, mm^{-1}	3.071	6.306
F(000)	1056.2	1424.0
2Θ range for data collection/°	3.14 to 25.00	5.02 to 55
Reflections collected	18 224	21 038
Independent reflections	4263 [$R_{int} = 0.0851$, $R_{sigma} = 2112$]	3006 [$R_{int} = 0.0363$, $R_{sigma} = 0.0273$]
Data/restraints/parameters	4263/0/258	3006/0/143
Goodness-of-fit on F^2	1.0311	1.070
Final R indices [$I > 2\sigma(I)$]^a	$R_1 = 0.0581$, w$R_2 = 0.1420$	$R_1 = 0.0328$, w$R_2 = 0.0647$
R Indices (all data)	$R_1 = 0.1230$, w$R_2 = 0.1898$	$R_1 = 0.0410$, w$R_2 = 0.0669$
Largest diff. peak/hole/e Å^{-3}	0.5650/−0.6818	1.13/−0.84

thermal stability. The polymer **1** is stable enough up to 290 °C then a major weight loss (75%) was observed from 290 °C to 360 °C followed by a minor weight loss (21%) till 540 °C due to the loss of ligand moieties and bromide ions, to produce the ZnSe residual mass (found, 4% and calculated, 10%; the less residual mass could be due to the unbalanced ratio of Se *vs.* Zn).

The solution state UV-vis absorbance spectra of $L \cdot H_2O$, and **1** were measured at room temperature in methanol solution (Fig. 5). The UV-vis absorption spectrum pattern of **1** comparable with $L \cdot H_2O$. Both $L \cdot H_2O$ and **1** gave a broad absorption band at 318 nm due to π–π* transitions.

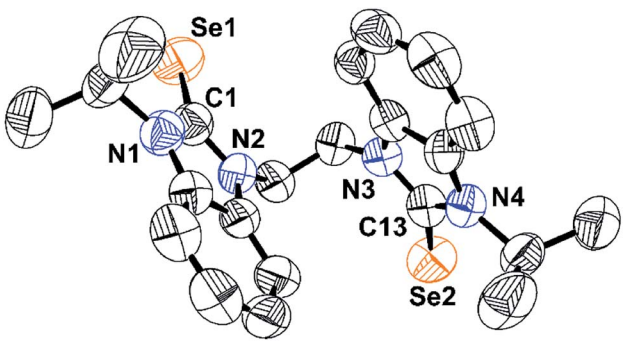

Fig. 1 The solid-state structure of $L \cdot H_2O$. The hydrogen atoms and water molecule have been eliminated for clarity. Selected bond lengths [Å] and bond angles [°] of $L \cdot H_2O$: C(1)–Se(1), 1.820(74), C(1)–N(1), 1.358(79), C(1)–N(2), 1.374(82), C(13)–Se(2), 1.837(65), C(13)–N(3), 1.366(65), C(13)–N(4), 1.356(65), N(1)–C(1)–N(2), 106.85(54), N(1)–C(1)–Se(1), 128.77(48), N(2)–C(1)–Se(1), 124.35(53), N(3)–C(13)–N(4), 107.51(46), N(3)–C(13)–Se(2), 125.11(49), N(4)–C(13)–Se(2), 127.36(38).

Catalyst 1 mediated Knoevenagel condensation

The construction of this new coordination polymer with Zn_2Se_2 units prompted us to study the catalytic activity of **1** in the Knoevenagel condensation reactions (Scheme 3). The Knoevenagel condensation reaction between activated methylene compounds and heterocyclic carbaldehyde is one of the most widely employed synthetic protocol to isolate the compounds with medicinal applications.[9]

Formally these reactions can be catalyzed by weak bases such as amines[10] or by Lewis acids[11] under homogeneous conditions, which always requires very high catalyst loading (around 40 mol%). Thus these protocols demand undesirable economic and environmental problems due to the corrosive nature of reaction waste or the difficulties in separating the catalysts. To overcome these issues, more-sustainable yet more-efficient catalysts are in great demand. Therefore several recyclable heterogeneous catalytic processes such as carbon nano-material,[12] silica[13] ionic liquid[14], or metal nano partial[15] based catalysts have been developed to satisfy the current requirements. In particular, the metal-based solid-state catalysts recently regained interest for low catalyst loading experiments.[16] However, to the best of our knowledge, the zinc-based Knoevenagel condensation reactions have never been reported as the zinc-based catalysts are more sustainable in nature.

Thus, the Knoevenagel condensation reaction between 8-hydroxyquinoline-2-carbaldehyde with ethyl-2-cyanoacetate has been investigated using catalyst **1**. 8-Hydroxy quinoline, and the corresponding derivative has great biological significance.[16] The condensation reaction between 8-hydroxyquinoline-2-carbaldehyde with ethyl-2-cyanoacetate was demonstrated

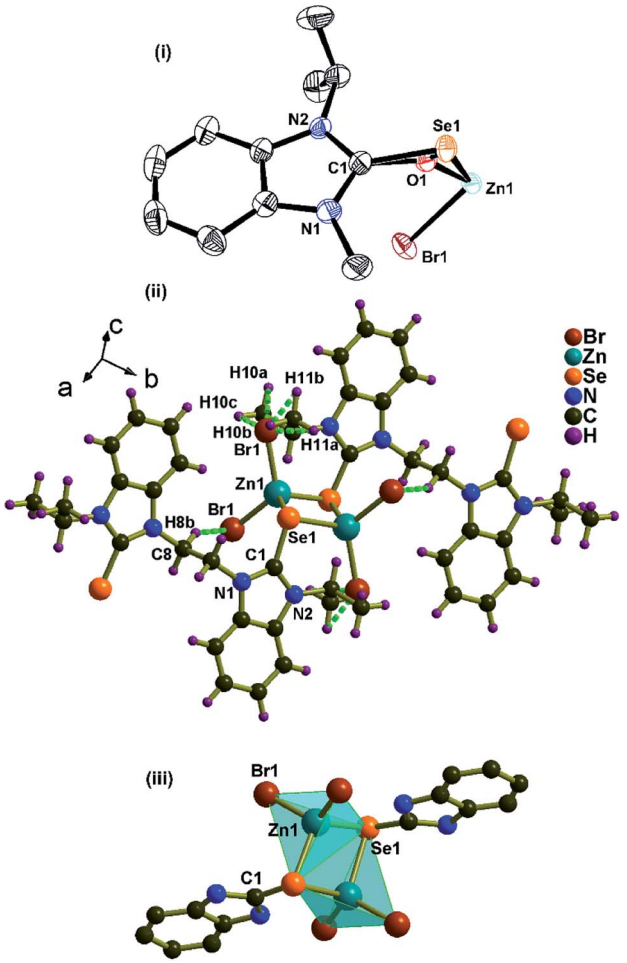

Fig. 2 (i) The asymmetric unit of **1**. Hydrogen atoms have been omitted for the clarity. (ii) The solid-state structure of **1**. The disordered atom next to selenium, assigned as oxygen with ~15% occupancy have been omitted for the clarity. (iii) The $Se_2Zn_2Br_4$ core of **1**. Selected bond lengths [Å] and bond angles [°] for **1**: Se(1)–Zn(1), 2.494(4), Zn(1)–Br(1), 2.367(4), Se(1)–C(1), 1.866(3), C(1)–Se(1)–Zn(1), 97.45(10), Br(1)–Zn(1)–Br(1), 121.56(3), Se(1)–Zn(1)–Se(1), 117.14(3).

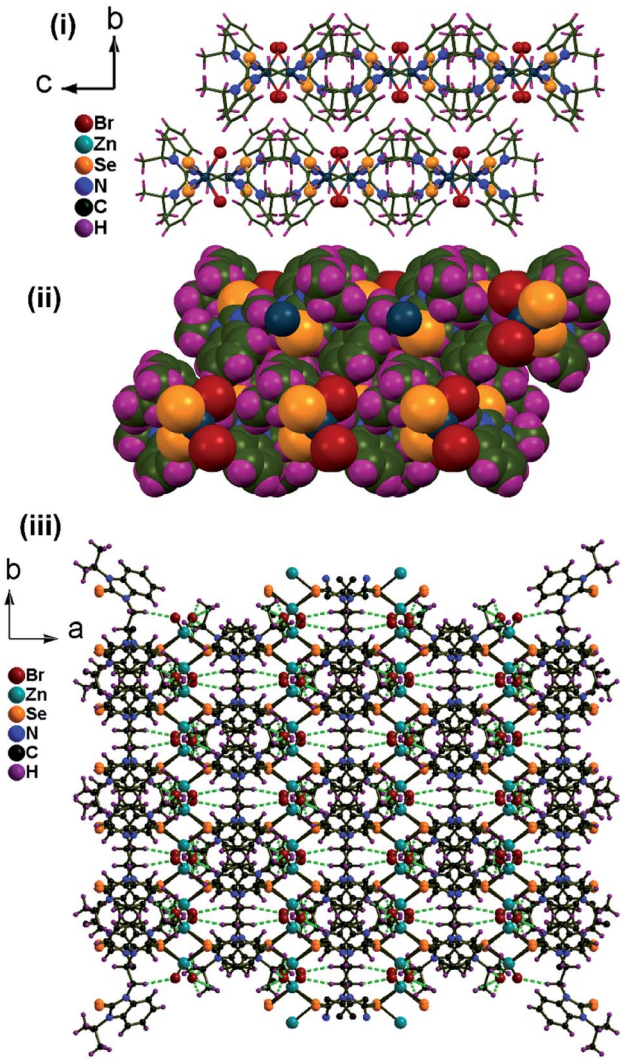

Fig. 3 (i) Arrangements of one-dimensional coordination polymers in **1** (view along *a* axis). (ii) Space-filling model of one-dimensional coordination polymers in **1** (view along *a* axis). (iii) Perspective view of the sheet structure of **1** through hydrogen bonding (view along the *c* axis).

using K_2CO_3 with poor yield (36%) in 1991.[17] As of now, there is no alternative synthetic methodology to perform this condensation reaction (based on SciFinder Search results in May 2020).

To evaluate the suitable catalytic condition, the reactions between 8-hydroxyquinoline-2-carbaldehyde and ethyl-2-cyanoacetate (1 : 1.1) was carried out using different solvents like DCM, $CHCl_3$, THF, Toluene, MeOH and EtOH under boiling condition (Table 2, entries 1–6). The polar to mid polar organic solvents such as THF, DCM, and $CHCl_3$ gave poor yield, while the polar-protic solvents such as EtOH and MeOH resulted in the better catalytic activity. Our attempts to use this catalyst under heterogeneous condition was not fruitful as the yield was poor. However, the excellent conversion was achieved using EtOH under homogenous conditions.

The reaction temperature was very much essential to achieve the targeted molecule within 1 h because the room temperature reaction gave a poor yield (30%) within 1 h or even after 24 h (41%). The optimization of catalyst loading experiment was next aimed. Decreasing the catalyst loadings from 5 mol% (yield 98%), 2 mol% (yield 96%), 1 mol% (yield 85%), to 0.5 mol% (yield 60%) did not allow full conversion. Indeed, the catalytic efficiency and stability of **1** could be attributed to the strong interaction between the imidazole selone, and the zinc center. This also leads to good efficiency in low catalyst loading. The rate of the reaction appeared particularly low with 2 mol% of precatalyst or $ZnBr_2$ or $\mathbf{L}\cdot H_2O$; even under reflux condition with 1 h reaction time could not allow the catalyst to reach the complete conversion.

The time conversion plot for the reaction between 8-hydroxyquinoline-2-carbaldehyde and ethyl-2-cyanoacetate in the presence of catalyst **1** is shown in Fig. 6. Under this optimized reaction condition, the reaction was over within 60 minutes. Interestingly, at such a low catalyst loading, the activity of **1** was comparable to diaminosilane-functionalized cobalt spinel ferrite ($CoFe_2O_4$) and MIL-53(Fe)@SiO_2@$NiFe_2O_4$ magnetic nanoparticles.[15a,b]

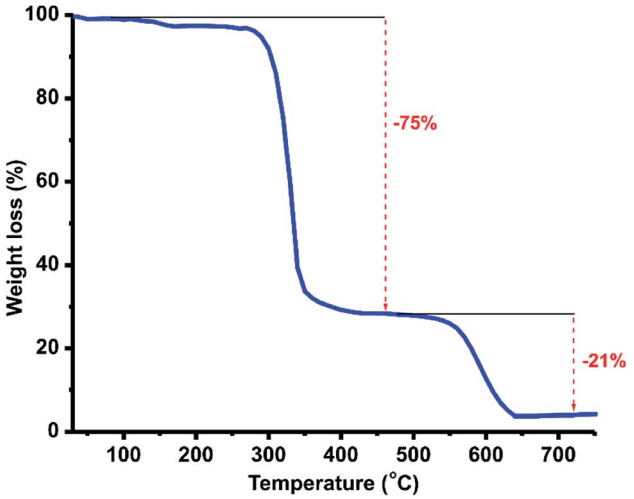

Fig. 4 TGA curve of **2** from 30 to 800 °C under a nitrogen atmosphere with a heating rate of 10 °C min^{-1}.

Based on the known catalytic pathways, a mechanism for the catalyst **1** mediated Knoevenagel condensation reaction has been proposed (Scheme 4).[9–17] We speculate that the aldehyde is activated by zinc(II) catalyst to generate the intermediate (**Ia**). The carbanion of ethyl-2-cyanoacetate attacks the electrophilic carbon on the zinc coordinated intermediate. The carbanionic character might be enhanced by the polar protic solvent such as ethanol, to favour the ketenimine intermediate (**Ia**).[18] The ketenimine intermediate (**Ia**) attacks the electrophilic Zn(II) intermediate to producing the intermediate (**Ib**) followed by the elimination of water molecules to yield the product.

Experimental

Materials and methods

All the manipulation was carried out under dry atmosphere. The solvents were purchased from commercial sources and used without further purification. Selenium powder (Sigma), sulphur

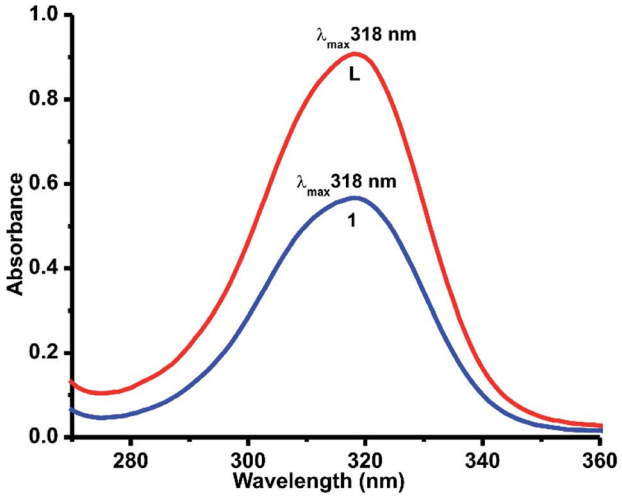

Fig. 5 Solution state UV-vis spectra of **L**·H_2O, and **1** in methanol at RT (2.9×10^{-5} M).

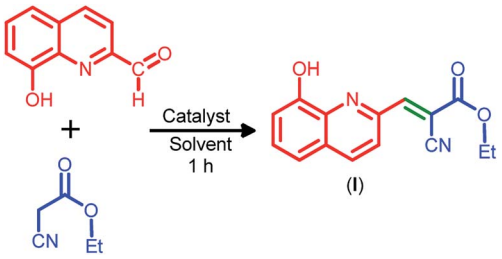

Scheme 3 Catalyst **1** mediated Knoevenagel condensation of 8-hydroxyquinoline-2-carbaldehyde with ethyl-2-cyanoacetate.

powder (Alfa Aesar), and $ZnBr_2$ (Sigma) were purchased and used as received. 1,1′-(Ethane)bis(3-isopropyl-benzimidazolium) bromide was synthesized as reported.[1c,3] FT-IR measurements (neat) was carried out on a Bruker Alpha-P Fourier transform spectrometer. Microanalyses of carbon, hydrogen, and nitrogen were carried out using a Euro EA – CHNSO Elemental Analyser. The UV-vis spectra were recorded on a T90+ UV-visible spectrophotometer. Thermogravimetric (TGA) analysis was performed using a TASDT Q600, Tzero-press. NMR spectra were recorded on Bruker Ultrashield-400 spectrometers at 25 °C unless otherwise stated. Chemical shifts are given relative to TMS and were referenced to the solvent resonances as internal standards. The crystal structures of **L**·H_2O and **1** were measured using the Oxford Supernova diffractometer. Single crystals obtained were mounted on Goniometer KM4/Xcalibur equipped with Sapphire2 (Large Be window) detector (CuKα radiation source, $\lambda = 1.5418$ Å). The single crystals of **L**·H_2O were obtained from their saturated solutions of chloroform, and layered with hexane at room temperature, while **1** was obtained from their saturated solution of acetonitrile and methanol mixture (1 : 1 ratio) at room temperature. Data were collected at 293 K for **L**·H_2O and 120 K for **1**. Using Olex2, the structure was solved with the Olex2.Solve, the structure solution program using charge flipping and refined with the Olex2.Refine

Table 2 The catalyst **1** mediated Knoevenagel condensation of 8-hydroxyquinoline-2-carbaldehyde with ethyl-2-cyanoacetate[a,b]

Entry	Solvent	Yield (%)
1	DCM	24
2	$CHCl_3$	26
3	THF	Trace
4	Toluene	22
5	MeOH	92
6	EtOH	96
7[c]	EtOH	30
8[d]	EtOH	60
9[e]	EtOH	85
10[f]	EtOH	98
11[g]	EtOH	28
12[h]	EtOH	0

[a] Reaction conditions: (0.10 mmol) 8-hydroxyquinoline-2-carbaldehyde, (0.10 mmol) ethyl-2-cyanoacetate, 2 mol% zinc(II) catalyst and 2 mL of solvent were used at reflux for 1 h. [b] Isolated yield after column chromatography. [c] Room temperature. [d] 0.5 mol%. [e] 1 mol%. [f] 5 mol%. [g] Catalyst: $ZnBr_2$. [h] Catalyst: **L**·H_2O.

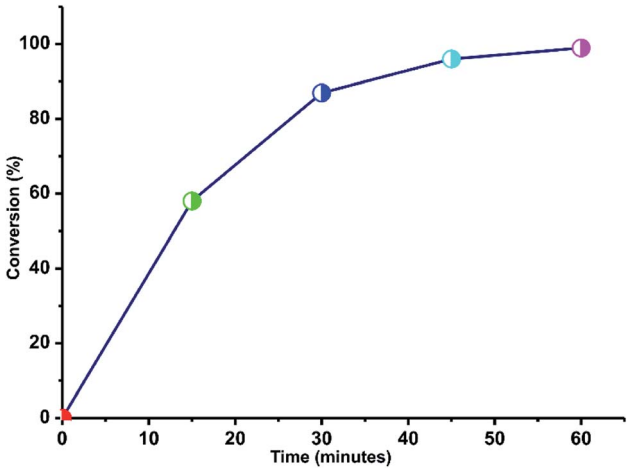

Fig. 6 Plot of time *vs.* yield for the reaction of 8-hydroxyquinoline-2-carbaldehyde and ethyl-2-cyanoacetate in ethanol at 70 °C.

refinement package using Gauss-Newton minimization.[19] Absorption corrections were performed on the basis of multi-scans. Non-hydrogen atoms were anisotropically refined. Hydrogen atoms were included in the refinement in calculated positions riding on their carrier atoms. No restraint has been made for any of the compounds. A solvent mask was calculated for **L**·H_2O and 36 electrons were found in a volume of 326 Å^3 in one void per unit cell. This is consistent with the presence of one water molecule per formula unit which accounts for 40 electrons per unit cell. Selenium atom in **1** is heavily disordered. Thus Se1 occupancy was refined freely and an unidentified "ghost" peak Q1 (2.4) next to Se was assigned as a freely occupied O atom. Se was refined to ~85% and O to ~15%. This suggests that there is a real disorder at selenium center. The resulting O–Zn distance of ~1.98 Å, as well as the C–O distance of ~1.51 Å, are quite reasonable. The O is out of the plane, which is not ideal. As a result R1 was decreased from 5.34% to 3.28%. However a final R1 of 3.28, and the position of oxygen close to a heavy element selenium with ~15% occupancy are challenging to determine. The present assessment should be convincing. Attempts to resolve the quality of data set of **1** by recrystallizing in the different solvent or conditions were not successful.

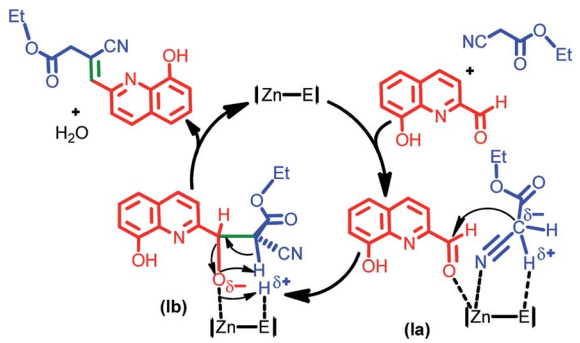

Scheme 4 Proposed catalytic mechanism for Zn(II) mediated Knoevenagel condensation reaction.

Synthesis of L·H_2O

To a mixture of potassium carbonate (1.194 g, 8.864 mmol), 1,1′-(ethane)bis(3-isopropyl-benzimidazolium) bromide (2.00 g, 3.93 mmol) and Se powder (0.683 g, 8.64 mmol), methanol (20 mL) was added. The reaction mixture was stirred at 70 °C for 24 h. The progress of the reaction was monitored by TLC. After completion of the reaction, the solvent was removed, water was added to the solid and extracted with dichloromethane (3 × 15 mL). The organic extract was washed with brine solution and dried over anhydrous Na_2SO_4. The organic extract was evaporated under reduced pressure to get analytically pure **L**. Yield: 76% (based on benzimidazolium salt). mp: 222–224 °C. Elemental analysis for $C_{22}H_{28}N_4OSe_2$ (522.40) (%): calcd C, 50.58; H, 5.40; N, 10.72; found C, 52.3; H, 5.1; N, 11.0. ^{1}H NMR ($CDCl_3$, 400.130 MHz): δ 1.56–1.59 (d, 12H, CH_3), 4.98 (s, 4H, CH_2), 5.83–5.88 (m, 2H, CH), 7.01–7.04 (t, 4H, Ar–H), 7.04–7.06 (m, 2H, Ar-CH), 7.42–7.45 (t, 2H, Ar–H). ^{13}C NMR ($CDCl_3$, 100.612 MHz): δ 164.8 (C=Se), 133.9 (Ar–C), 130.6 (Ar–C), 123.0 (Ar–C), 122.7 (Ar–C), 110.8 (Ar–C), 110.0 (Ar–C), 51.5 (N–CH_2), 43.9 (N–CH), 20.0 (CH_3). FT-IR (neat) $\bar{\upsilon}$: 2934(w), 1700(m), 1448(m), 1398(s), 1331(s), 1250(m), 1164(s), 1082(s), 736(s), 562(m) cm^{-1}.

Synthesis of 1

To a stirred solution of $ZnBr_2$ (0.133 g, 0.59 mmol) in toluene, **L**·H_2O (0.10 g, 0.59 mmol) was added. The reaction mixture was stirred at room temperature for 3 days to yield the off white precipitate. The solvent was removed then the solid residue was washed with hexane (2 × 5 mL) and dried under a high vacuum. The resulting solid was dissolved in acetonitrile and methanol mixture (1 : 1 ratio) to obtain colorless crystals of **1** at 25 °C. Yield: 75% (based on $ZnBr_2$). Elemental analysis for $C_{22}H_{26}Br_2N_4Se_2Zn$ (729.58) (%): calcd. C, 36.22; H, 3.59; N, 7.68; found C, 36.1; H, 3.5; N, 7.6. ^{1}H NMR (DMSO-d_6, 400.130 MHz): δ 1.45–1.63 (d, 6H, CH_3), 4.87 (s, 2H, CH_2), 5.56–5.61 (m, 1H, CH), 7.01–7.09 (m, 3H, Ar–H), 7.50–7.52 (d, 1H, Ar–H). ^{13}C NMR (DMSO-d_6, 100.612 MHz): δ 133.3 (Ar–C), 130.1 (Ar–C), 122.7 (Ar–C), 122.6 (Ar–C), 111.1 (Ar–C), 50.9 (N–CH_2), 43.6 (N–CH), 19.3 (CH_3) (C=Se signal is absent due to poor solubility of **1**). FT-IR (neat) $\bar{\upsilon}$: 2985(m), 1615(m), 1457(w), 1413(s), 1260(m), 1135(m), 1091(m), 753(s), 567(w) cm^{-1}.

Procedure for Knoevenagel condensation reactions

To a mixture of 8-hydroxyquinoline-2-carbaldehyde (1.0 equiv.), ethyl-2-cyanoacetate (1.0 equiv.), and Zn(II) catalyst **1** (2 mol%), ethanol (2 mL) was added. The reaction mixture was heated under reflux for 1 h. The progress of the reaction was monitored by TLC then the solvent was removed. The crude product was redissolved in hexane. The desired product was purified by column chromatography using EtOAc/hexane (1 : 9).

Conclusions

A novel one-dimensional (1D) coordination polymer, [(**L**)$Zn(Br)_2]_2$ (**1**) (**L** = 3,3′-ethane-1,2-diyl)-bis(1-isopropyl-1*H*-benzo[*d*]imidazole-2(3*H*)-selenone), was isolated through a reaction of zinc bromide with **L**·H_2O at room temperature. The X-ray crystallography for **1** revealed that the zinc center of the

compound depicted a tiny Zn_2Se_2 ring system linked by a diselone ligand to construct a 1D chain structure. This result implies that the spacer of the imidazole-selone ligands has a significant effect on the network motifs of the coordination frameworks. The coordination polymer **1** was used as a catalyst in the synthesis of substituted 8-hydroxy-2-quinolinyl derivative through Knoevenagel condensation reaction with very low catalyst loading. This represents the first zinc(II) coordination polymer mediated Knoevenagel condensation reaction. The advancement of this catalytic protocol is in progress.

Conflicts of interest

There are no conflicts to declare.

Acknowledgements

GP gratefully acknowledge DST-SERB (EMR/2017/001211) for financial support. MM thank CSIR-SRF for the fellowship.

Notes and references

1 (*a*) K. Srinivas, P. Suresh, C. N. Babu, A. Sathyanarayana and G. Prabusankar, *RSC Adv.*, 2015, **5**, 15579–15590; (*b*) K. Srinivas, C. N. Babu and G. Prabusankar, *Dalton Trans.*, 2015, **44**, 15636–15644; (*c*) K. Srinivas, A. Sathyanarayana, C. N. Babu and G. Prabusankar, *Dalton Trans.*, 2016, **45**, 5196–5209; (*d*) K. Srinivas and G. Prabusankar, *RSC Adv.*, 2018, **8**, 32269–32282; (*e*) G. Prabusankar, A. Mannem and N. Muthukumaran, *J. Organomet. Chem.*, 2019, **884**, 29–35; (*f*) R. Karupnaswamy, M. Mannarsamy, M. Vaddamanu and G. Prabusankar, *Eur. J. Inorg. Chem.*, 2019, 4902–4907.

2 (*a*) W. G. Jia, Y. B. Huang, Y. J. Lin and G. X. Jin, *Dalton Trans.*, 2008, 5612–5620; (*b*) H. R. Kim, I. G. Jung, K. Yoo, K. Jang, E. S. Lee, J. Yun and S. U. Son, *Chem. Commun.*, 2010, **46**, 758–760; (*c*) E. Alvarado, A. C. Badaj, T. G. Larocque and G. G. Lavoie, *Chem.–Eur. J.*, 2012, **18**, 12112–12121; (*d*) J. Jin, H. W. Shin, J. H. Park, J. H. Park, E. Kim, T. K. Ahn, D. H. Ryu and S. U. Son, *Organometallics*, 2013, **32**, 3954–3959; (*e*) Y. F. Han, L. Zhang, L. H. Weng and G. X. Jin, *J. Am. Chem. Soc.*, 2014, **136**, 14608–14615; (*f*) N. Ghavale, S. T. Manjare, H. B. Singh and R. J. Butcher, *Dalton Trans.*, 2015, **44**, 11893–11900; (*g*) G. K. Rao, A. Kumar, J. Ahmed and A. K. Singh, *Chem. Commun.*, 2010, **46**, 5954–5956; (*h*) C. Fleckenstein, S. Roy, S. Leuthaeusser and H. Plenio, *Chem. Commun.*, 2007, 2870–2872; (*i*) C. Zhang and M. L. Trudell, *Tetrahedron Lett.*, 2000, **41**, 595–598.

3 K. Srinivas and G. Prabusankar, *Dalton Trans.*, 2017, **46**, 16615–16622.

4 C. N. Babu, K. Srinivas and G. Prabusankar, *Dalton Trans.*, 2016, **45**, 6456–6465.

5 (*a*) G. Prabusankar, M. Vaddamanu and K. Velappan, *New J. Chem.*, 2020, **44**, 129–140; (*b*) M. Vaddamanu and G. Prabusankar, *Eur. J. Inorg. Chem.*, 2020, **25**, 2403–2407; (*c*) M. Vaddamanu, R. Karupnaswmy, K. Srinivas and G. Prabusankar, *ChemistrySelect*, 2016, **1**, 4668–4671; (*d*) G. Prabusankar, A. Sathyanarayana, K. Srinivas, P. Suresh and I. Nath, *ChemistrySelect*, 2018, **3**, 1294–1299; (*e*) R. Karupnaswamy and G. Prabusankar, *J. Chem. Sci.*, 2018, **130**, 1–7.

6 M. Vaddamanu, K. Velappan and G. Prabusankar, *New J. Chem.*, 2020, **44**, 3574–3583.

7 (*a*) G. Prabusankar, G. Raju, M. Vaddamanu, N. Muthukumaran, A. Sathyanarayana, S. Y. Nakamura, Y. Masaya, K. Hisano, O. Tsutsumi, C. Biswas and S. S. K. Raavi, *RSC Adv.*, 2019, **9**, 14841–14848; (*b*) A. Beheshti, M. B. Pour, C. T. Abrahams and H. Motamedi, *Polyhedron*, 2017, **135**, 258–264.

8 For selected examples: (*a*) R. M. Balleste, J. G. Herrero and F. Zamora, *Chem. Soc. Rev.*, 2010, **39**, 4220–4233; (*b*) C. Janiak, *Dalton Trans.*, 2003, 2781–2804; (*c*) B. Bhattacharya, A. A. L. Michalchuk, D. Silbernagl, M. Rautenberg, T. Schmid, T. Feiler, K. Reimann, A. Ghalgaoui, H. Sturm, B. Paulus and F. Emmerling, *Angew. Chem., Int. Ed.*, 2020, **59**, 5557–5561; (*d*) R. Aoki, R. Toyoda, J. F. Kogel, R. Sakamoto, J. Kumar, Y. Kitagawa, K. Harano, T. Kawai and H. Nishihara, *J. Am. Chem. Soc.*, 2017, **139**, 16024–16027; (*e*) C. Hermosa, J. V. Alvarez, M. R. Azani, C. J. G. Garcia, M. Fritz, J. M. Soler, J. G. Herrero, C. G. Navarro and F. Zamora, *Nat. Commun.*, 2013, 4; (*f*) G. Givaja, P. Amo-Ochoa, C. J. Gomez-Garcia and F. Zamora, *Chem. Soc. Rev.*, 2012, **41**, 115–147; (*g*) Z. Chen, D. Luo, M. Kang and Z. Lin, *Inorg. Chem.*, 2011, **50**, 4674–4676; (*h*) Y. Song, L. Yu, Y. Gao, C. Shi, M. Cheng, X. Wang, H. J. Liu and Q. Liu, *Inorg. Chem.*, 2017, **56**, 11603–11609.

9 (*a*) F. Freeman, *Chem. Rev.*, 1981, **80**, 329–350; (*b*) L. F. Tietze, *Chem. Rev.*, 1996, **96**, 115–136; (*c*) M. M. Heravi, F. Janati and V. Zadsirjan, *Monatsh. Chem.*, 2020, **151**, 439–482.

10 (*a*) H. P. Collin, L. Gustavo, L. Guimaraes, M. S. Valle and J. R. Pliego, *J. Phys. Chem. B*, 2017, **121**, 5300–5307; (*b*) A. Erkkila, I. Majander and P. M. Pihko, *Chem. Rev.*, 2007, **107**, 5416–5470; (*c*) J. Zhu, F. Wang, D. Li, J. Zhai, P. Liu, W. Zhang and Y. Li, *Catal. Lett.*, 2020, **150**, 1909–1922.

11 For selected examples: (*a*) A. Dandia, V. Parewa, A. K. Jain and K. S. Rathore, *Green Chem.*, 2011, **13**, 2135–2145; (*b*) Y. Ogiwara, K. Takahashi, T. Kitazawa and N. Sakai, *J. Org. Chem.*, 2015, **80**, 3101–3110; (*c*) K. Yamashita, T. Tanaka and M. Hayash, *Tetrahedron*, 2005, **61**, 7981–7985; (*d*) G. Bartoli, M. Bosco, A. Carlone, R. Dalpozzo, P. Galzerano, P. Melchiorre and L. Sambri, *Tetrahedron Lett.*, 2008, **49**, 2555–2557; (*e*) J. S. Yadav, D. C. Bhunia, V. K. Singh and P. Srihari, *Tetrahedron Lett.*, 2009, **50**, 2470–2473; (*f*) V. Srinivas and M. Koketsu, *J. Org. Chem.*, 2013, **78**, 11612–11617.

12 (*a*) H. Wang, C. Wang, Y. Yang, M. Zhao and Y. Wang, *Catal. Sci. Technol.*, 2017, **7**, 405–417; (*b*) P. Sharma and Y. Sasson, *RSC Adv.*, 2017, **7**, 25589–25596; (*c*) G. Tuci, L. Luconi, A. Rossin, E. Berretti, H. Ba, M. Innocenti, D. Yakhvarov, S. Caporali, C. Pham-Huu and G. Giambastiani, *ACS Appl. Mater. Interfaces*, 2016, **8**, 30099–30106.

13 M. Shirotori, S. Nishimura and K. Ebitani, *J. Mater. Chem. A*, 2017, **5**, 6947–6957.

14 (*a*) I. Hierro, Y. Pérez and M. Fajardo, *Mol. Catal.*, 2018, **450**, 112–120; (*b*) K. P. Boroujeni and M. Jafarinasab, *Chin. Chem. Lett.*, 2012, **23**, 1067–1070; (*c*) D. Elhamifar and S. Kazempoor, *J. Mol. Catal. A: Chem.*, 2016, **415**, 74–85.

15 (*a*) N. Yao, J. Tan, Y. Liu and Y. L. Hu, *Synlett*, 2019, **30**, 699–702; (*b*) N. T. S. Phan and C. W. Jones, *J. Mol. Catal. A: Chem.*, 2006, **253**, 123–131; (*c*) V. S. R. Pullabhotla, A. Rahman and S. B. Jonnalagadda, *Catal. Commun.*, 2009, **10**, 365–369; (*d*) B. Şen, E. H. Akdere, A. Şavk, E. Gultekin, O. Paral, H. Goksu and F. Şen, *Appl. Catal., B*, 2018, **225**, 148–153; (*e*) *Supported Catalysts and their Applications*, ed. D. B. Jackson, D. J. Macquarrie, J. H. Clark, D. C. Sherrington and A. P. Kybett, RSC, Cambridge, 2001, p. 203; (*f*) K. Yamashita, T. Tanaka and M. Hayashi, *Tetrahedron*, 2005, **61**, 7981–7985.

16 Selected Example: (*a*) A. Basak, Y. Abouelhassan, V. M. Norwood, F. Bai, M. T. Nguyen, S. Jin and R. W. Huigens, *Chem.–Eur. J.*, 2016, **22**, 9181–9189; (*b*) C. Deraeve, C. Boldron, A. Maraval, H. Mazarguil, H. Gornitzka, L. Vendier, M. Pitie and B. Meunier, *Chem.–Eur. J.*, 2008, **14**, 682–696; (*c*) R. Suresh, S. Muthusubramaniyan, R. Senthilkumaran and G. Manickam, *J. Org. Chem.*, 2012, **77**, 1468–1476; (*d*) L. B. Freitas, T. F. Borgata, R. P. Freitas, A. L. Ruiz, G. M. Marchetti, J. E. Carvalho, E. F. Cunha, T. C. Ramalho and R. B. Alves, *Eur. J. Med. Chem.*, 2014, **84**, 595–604.

17 C. Su, Z. C. Chen and Q. Zheng, *Synthesis*, 2003, **4**, 555–559.

18 (*a*) L. J. Bourhis, O. V. Dolomanov, R. J. Gildea, J. A. K. Howard and H. Puschmann, *Acta Crystallogr., Sect. A: Found. Adv.*, 2015, **71**, 59–75; (*b*) O. V. Dolomanov, L. J. Bourhis, R. J. Gildea, J. A. K. Howard and H. Puschmann, *J. Appl. Crystallogr.*, 2009, **42**, 339–341.

19 (*a*) L. J. Bourhis, O. V. Dolomanov, R. J. Gildea, J. A. K. Howard and H. Puschmann, *Acta Crystallogr., Sect. A: Found. Adv.*, 2015, **71**, 59–75; (*b*) O. V. Dolomanov, L. J. Bourhis, R. J. Gildea, J. A. K. Howard and H. Puschmann, *J. Appl. Crystallogr.*, 2009, **42**, 339–341.